

## Research article

# Loss of Slc39a12 in hippocampal neurons is responsible for anxiety-like behavior caused by temporomandibular joint osteoarthritis

Zhenguo Shen<sup>a,1</sup>, Chenyu Fan<sup>a,1</sup>, Chunmeng Ding<sup>a</sup>, Mengyue Xu<sup>a</sup>, Xian Wu<sup>b</sup>,  
Yuanyin Wang<sup>a,\*\*</sup>, Tian Xing<sup>a,\*</sup>

<sup>a</sup> College & Hospital of Stomatology, Anhui Medical University, Key Lab. of Oral Diseases Research of Anhui Province, Hefei, 230032, China

<sup>b</sup> Anhui Province Key Laboratory of Major Autoimmune Diseases, Anhui Institute of Innovative Drugs, School of Pharmacy, Anhui Medical University, Hefei, 230032, China

## ARTICLE INFO

## Keywords:

Anxiety  
Oxidative stress  
Slc39a12  
Temporomandibular joint  
Osteoarthritis

## ABSTRACT

**Background:** An evident association between mood disorders and TMJ dysfunction has been demonstrated in previous studies. This study observed both the behavioral changes and the pathological changes in hippocampal tissue of rats in an animal model of TMJ-OA by injecting MIA into TMJ.

**Methods:** Eighteen SD rats were randomly assigned to the NC group and the MIA groups. A TMJ-OA model was established to assess the HWT in the TMJ region, and the rats were subjected to the OFT and EPM. HE, O-fast green staining, qRT-PCR and immunofluorescence were used to detect condylar damage. Serum and hippocampal oxidative stress levels were detected. Functions of genes obtained by RNA-Seq were investigated using H<sub>2</sub>O<sub>2</sub>, ZnCl<sub>2</sub> and transfection of siRNA on HT22 cells.

**Results:** Injection of MIA resulted in disorganization of the chondrocyte layer on the condylar surface of rats, with reduced synthesis and increased degradation of the condylar cartilage matrix and reduced HWT. The results of the OFT and EPM showed that the rats in the MIA group developed anxiety-like behavior during the sixth week of MIA injection. Increased Nox4 expression, decreased SOD2 expression, elevated MDA level, and reduced GSH level were detected in serum and hippocampal neurons in the MIA group, with nuclear pyknosis and reduced Nissl bodies observed in neurons. The expression of Slc39a12 in hippocampal neurons of rats in the MIA group decreased. Slc39a12 knockdown in HT22 cells induced increased Nox4 expression, decreased SOD2 expression, increased MDA level, and reduced GSH and intracellular Zn<sup>2+</sup>. Oxidative stress in HT22 cells after transfection and H<sub>2</sub>O<sub>2</sub> stimulation was reversed when ZnCl<sub>2</sub> was added.

**Abbreviations:** CFA, complete Freund's adjuvant; CUMS, chronic unpredictable mild stress; EPM, elevated plus maze test; GSH, glutathione; HE, hematoxylin and eosin; ICP-MS, inductively coupled plasma mass spectrometry; MDA, malondialdehyde; MIA, sodium iodoacetate; HWT, head withdrawal threshold; NC, negative control; Nox, NADPH oxidase; OA, osteoarthritis; OFT, open field test; siRNA, small interfering RNA; Slc39a12, solute carrier family 39 member 12; SOD2, superoxide dismutase 2; TMD, temporomandibular disorders; TMJ, temporomandibular joint; UAC, unilateral anterior crossbite.

\* Corresponding author.

\*\* Corresponding author.

E-mail addresses: [wyy1970548@sohu.com](mailto:wyy1970548@sohu.com) (Y. Wang), [xingtian8110@163.com](mailto:xingtian8110@163.com) (T. Xing).

<sup>1</sup> Zhenguo Shen and Chenyu Fan contribute equally to this work.

<https://doi.org/10.1016/j.heliyon.2024.e26271>

Received 23 November 2023; Received in revised form 7 February 2024; Accepted 9 February 2024

Available online 10 February 2024

2405-8440/© 2024 Published by Elsevier Ltd.

This is an open access article under the CC BY-NC-ND license

(<http://creativecommons.org/licenses/by-nc-nd/4.0/>).

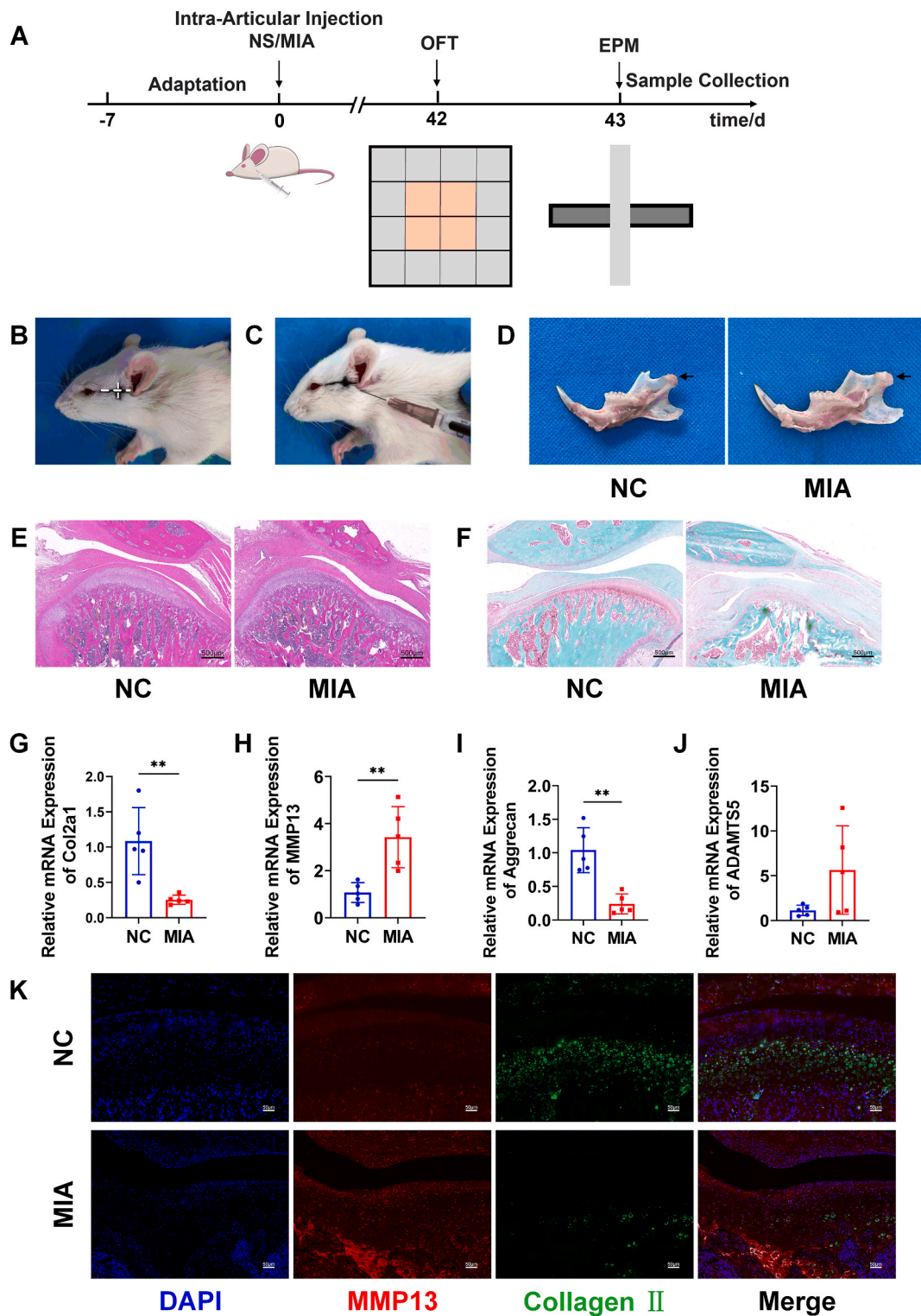


**Fig. 1.** MIA injection induced TMJ-OA.

(A) In vivo experimental flow chart. (B) Marking point on the body surface of rat condyle. (C) Schematic diagram of insertion point and direction of MIA injection. (D) Macroscopical view of rat condyle. (E) HE staining of TMJ. (F) Safranin O-fast green staining of TMJ. (G–J) Relative mRNA expression of Col2a1, MMP13, Aggrecan, and ADAMTS5 in condylar cartilage. (K) Immunofluorescence staining of MMP13 (red) and Collagen II (green) in condylar cartilage. All data were mean  $\pm$  SD,  $n = 5$ ,  $**p < 0.01$  vs. NC. (For interpretation of the references to color in this figure legend, the reader is referred to the Web version of this article.)

**Conclusion:** Loss of Slc39a12 in hippocampal neurons results in cellular oxidative stress, further leading to neuronal damage. This may potentially explain how TMJ-OA triggers anxiety-like behavior in rats.

## 1. Introduction

Temporomandibular disorders (TMD) are a range of diseases affecting the masticatory muscles, temporomandibular joint (TMJ) and associated structures, which can cause discomfort and/or dysfunction of maxillofacial region. Approximately 31% of adults or elderly people suffer from TMD [1]. Since the late 20th century, several researches have shown that TMD patients usually experience pain, disability and diminished quality of life [2]. Specifically, self-reported jaw masticatory function declines and general somatic symptoms and pressure pain sensitivity in the orofacial region increase. TMD have been evaluated clinically from physiological and psychological perspectives, and both pharmacological and behavioral treatments can be taken into account at the same time [3].

One subtype of TMD is osteoarthritis of the temporomandibular joint (TMJ-OA), with a high incidence of 40% in TMD patients [4]. TMJ-OA is characterized by focal excessive cartilage degeneration with subchondral bone erosion, sclerosis, and remodeling, as well as persistent synovial inflammation [5]. The primary goals of treating TMJ-OA are directed at decreasing related-pain and disability, decelerating future disease progression, and restoring TMJ function. Most of the therapy is confined to symptomatic treatment options in clinical practice, however, in view of the uncertain etiology of the disease and irreversible damage [6]. Consequently, the prolonged treatment cycle and partially effective response may considerably affect the patient's daily activities and quality of life of patients [7, 8], accompanied by mood disorders like anxiety, fear, stress, anger or depression [9–11]. This is a major challenge for clinicians and a phenomenon worth talking about.

The use of appropriate animal models helps to disclose the pathogenesis by which TMJ-OA may play a role in psychiatric disorders, providing clues for possible interventions. Currently, chemical, mechanical, and surgical methods can be used to construct TMJ-OA models in rats or mice, among which the most commonly used is intra-articular injection of chemical agents [12]. MIA, as one of the main injected chemical agents, can cause pathological changes in arthritis models similar to those in clinical OA patients, and the established rat TMJ-OA model has been proved reproducible and reliable in several studies [13,14].

The hippocampus, as a major part of the limbic system [15], plays vital roles in memory, cognition, spatial and situational processing, and emotional regulation, all of which affect mental health. Emotional abnormalities were described as associated with the disorganization of processing or changes in synaptic plasticity in hippocampus. In a type of chronic orofacial injury, burning mouth syndrome also showed a crucial regulatory effect of the hippocampus on emotional symptoms.

Meanwhile, as a common physiological phenomenon in eukaryotes, oxidative stress refers to a state of excessive production of reactive oxygen species and the reduced antioxidant function. Excessive oxidative stress damages DNA, RNA, and proteins, disrupting the normal structure and function of cells and triggering several diseases, including mood disorders [16].

Previous studies suggest that oxidative stress in hippocampus generates disturbances in neurotransmission that affect neuronal functioning and overall brain activity. In addition, this stress can also impact on membrane integrity through lipid peroxidation, decreasing membrane fluidity and protein activity, and leading to neuronal death ultimately.

Interestingly, the current mechanisms underlying the association between TMJ-OA and mood disorders, especially the changes in cellular regulation within hippocampus along temporomandibular inflammatory injury have remained underexplored. This study aimed to establish a TMJ-OA model by injecting MIA into the TMJ of rats and investigating their emotional performance through behavioral tests. By selecting hippocampus as the research center, we examined the possible mechanisms behind the correlation between TMJ-OA and mood disorders, and proposed future clinical treatment and prevention strategies.

## 2. Material and methods

### 2.1. Animals

The male SD rats, aged 6 weeks, were acquired from Liaoning Changsheng Biotechnology Co., Ltd (Liaoning, China). All procedures followed the care standards for laboratory animals and had been approved by the Laboratory Animal Ethics Committee of Anhui Medical University (LLSC20221097). Animals were kept in a standard environment of 22–25 °C, 12 h light and dark cycle, 40–60% relative humidity.

### 2.2. TMJ-OA model

Eighteen SD rats were randomly divided into NC and MIA groups (n = 9 per group). A small animal anesthesia machine was used with a mixture of 3% isoflurane (RDW, China) and 97% air for anesthesia induction, followed by a 2% isoflurane mask for maintenance. To induce TMJ-OA, 50  $\mu$ L of 10 mg/mL MIA (Sigma-Aldrich, USA) dissolved in isotonic sodium chloride solution (NS) was bilaterally injected into the sub-articular cavities of rats (Fig. 1B and C). The NC group received only sterile NS. Bilateral TMJ injections of NS or MIA in rats were recorded as day 0. The open field test (OFT) was performed on day 43 of model construction, and elevated plus maze test (EPM) was performed on day 44, followed by animal tissue sampling (Fig. 1A).

### 2.3. Animal behavior tests

Each animal was acclimatized to the experimental environment for at least 1 h prior to behavioral testing. Following the detection of each animal, the excreted feces were meticulously wiped and dried with 75% alcohol cotton balls to prevent any impact on the results due to odor or foreign bodies before testing the next animal. Electric VonFrey (IITC, USA) and Visu Track (Xinruan, China) were used to record and analyze the behavior of each animal.

#### 2.3.1. Head withdrawal threshold (HWT) measurement

To test HWT, the rat was cupped in the palm of the hand by one of the experimenters, with restriction of its lower limb movement and free movement of its forelimbs and head. The skin in TMJ region of the rat was stimulated with a rigid tip connected to the Electric VonFrey, and values were recorded when the rat hissed, avoided, scratched, or attacked. Each rat was tested five times at intervals of a few seconds on each side, and the results were shown as the average of ten different test values. HWT was recorded on day 1 prior to MIA injection as the baseline (BL), and on days 1, 3, 5, 7 and 14 after injection. In order to maintain consistency in assessing behavioral responses, all behavioral observations were conducted by a single experimenter, unaware of the experimental conditions.

#### 2.3.2. Open field test (OFT)

The experimental apparatus consisted of a large roofless box with dimensions of  $100 \times 100 \times 40$  cm, which was divided into two areas. The  $50 \times 50$  cm area in the center was called the central area, and the other fell into peripheral areas. Rats were gently placed in the central area and allowed to move freely for 5 min. The trajectory of each rat was recorded and analyzed; the total distance moved and the distance moved in the central area were calculated.

#### 2.3.3. Elevated plus maze test (EPM)

A cross-shaped platform placed 60 cm above the ground was used. It was composed of two open ( $45 \times 10$  cm) and two closed arms ( $50 \times 10$  cm). The closed walls were 40 cm high. At the beginning of the experiment, the rats were gently placed in the center of the maze and allowed to freely explore their environment for 5 min. The trajectory of each rat was recorded and analyzed to determine the total movement distance and open arm movement distance.

### 2.4. Tissue sampling

Rats were euthanized by administering an isoflurane overdose. Following this procedure, blood was collected from the heart tip of the rats, and the serum was obtained by centrifugation at 3000r/min for 15min after standing at room temperature for 40min. Then NS was injected into the heart to facilitate rapid blood drainage. The rats were then decapitated, split in half, and the condyles were exposed. Lastly, the entire bilateral TMJ was carefully dissected for further experimental procedures. A midline incision was then made to expose the brain. The rat brain tissue, including both the left and right hippocampus, was promptly isolated on ice and preserved at  $-80^{\circ}\text{C}$  in a cryogenic refrigerator as per the Brainmaps 4.0 atlas until future analysis [17].

### 2.5. Histopathological staining

TMJ tissue harvested from each group of rats was fixed in 4% paraformaldehyde for 48 h and subsequently immersed in decalcifying fluid for 12 weeks, with the fluid replaced twice a week. Following decalcification, the TMJ tissue was sliced into  $4\ \mu\text{m}$  in thickness after gradient dehydration and embedding. The TMJ tissue sections were then deparaffinized and stained with hematoxylin and eosin (HE) and safranin O-fast green. The hippocampus tissue was soaked in 4% paraformaldehyde for 48 h, dehydrated, embedded, and cut into  $4\ \mu\text{m}$ -thick slices. The acquired slices were deparaffinized and stained with HE and Nissl. Subsequently, a gradient of xylene was used for dehydration before sealed with a neutral resin. Lastly, the pathological sections were examined under a photographic microscope (Leica, Germany).

### 2.6. RNA-seq and data analysis

The RNA-Seq method for transcriptomics was in line with the research team's previous research report [18]. Differences in gene expression were analyzed using DESeq (version 1.30.0) with the following screening conditions: Basemean  $>10$ , expression difference multiple  $|\log_2\text{FoldChange}| > 1$ , significant p-value  $<0.05$ .

### 2.7. Quantitative real-time PCR (q-PCR)

Tissue and cells' total RNA extraction and q-PCR methods were in line with the research team's previous research report [18]. A LC96 real-time fluorescence quantitative PCR instrument was used for amplification and analysis. Using  $\beta$ -actin as the internal reference, the final result was calculated using the  $2^{-\Delta\Delta\text{Ct}}$  method. The primer sequences used for detection were listed in [Supplementary Table 1](#).

## 2.8. Western blot

Tissue and cells' protein extraction and Western blot methods were in line with the research team's previous research report [18]. Protein bands were detected by chemiluminescence using an ECL system. Primary and secondary antibody removal solutions (Beyotime, China) were used to eliminate antibodies present on the nitrocellulose membrane. The primary and secondary antibodies were then re-blocked and incubated to detect protein band signals. Quantification of the results was performed using ImageJ software (National Institutes of Health). Primary antibodies targeting Slc39a12 (1:500; HUABIO, China), Nox4 (1:800; Zen-Bioscience, China), SOD2 (1:1000; Proteintech, China), and  $\beta$ -actin (1:3000; Proteintech, China) were used. HRP-conjugated goat anti-rabbit (1:7500; ZSGB, China) and HRP-conjugated goat anti-mouse antibodies (1:7500; ZSGB, China) were employed for the subsequent analysis.

## 2.9. Immunofluorescence staining

The paraffin sections were dewaxed. The antigen was obtained by heating the EDTA solution in a microwave for 10 min. The cells that propagated on climbing plates required fixation with 4% paraformaldehyde for 15 min and did not require repair antigens. The slices were sealed with an immunostaining sealing solution (Beyotime, China) for 10 min at 22–25 °C. The slices were then washed three times for 10 min each and subsequently maintained at 4 °C for 16 h using the MMP13 antibody (1:150; Proteintech, China), Collagen II antibody (1:100; Abcam, USA), Slc39a12 antibody (1:80) or NeuN antibody (1:100; Proteintech, China). The sections were rinsed three times with PBS-T and then incubated with a fluorescent secondary antibody at a 1:100 dilution for 2 h. After sealing the cross-sections with an anti-fluorescence quenching reagent containing DAPI, the results were observed and photographed using a fluorescent microscope (Motic, China).

## 2.10. HT22 cells culture and exposure to H<sub>2</sub>O<sub>2</sub>

HT22 cells from mouse hippocampal neurons were sponsored by Professor Deyong Chu of Anhui Medical University. These cells were cultured with DMEM high glucose medium (Gibco, USA) containing 10% fetal bovine serum and 100 U/ml penicillin-streptomycin at 37 °C under a humidified atmosphere of 95% air and 5% CO<sub>2</sub>. The culture dish was subcultured after the confluence rate reached 80–90%, using a specialized culture medium for all subsequent experiments. To verify the role of Zn<sup>2+</sup> in the process of oxidative stress occurring in neurons, we divided HT22 cells into three groups and cultured them for 72h using dedicated medium, medium with 200  $\mu$ mol/L H<sub>2</sub>O<sub>2</sub> added, and medium with 200  $\mu$ mol/L H<sub>2</sub>O<sub>2</sub> added and mixed with 2  $\mu$ mol/L ZnCl<sub>2</sub>.

## 2.11. Transfection of HT22 cells with siRNA

Small interfering RNA (siRNA) was designed and synthesized by HANBIO Technology (Shanghai, China) to target Slc39a12. The sequences of the Slc39a12 siRNAs (mouse) were as follows: sense, 5'-CCACCACUCUGGAGAAAUATT-3' and antisense, 5'-UAUUU-CUCCAGAGUGGUGGTT-3'. Negative scrambled siRNAs (sense, 5'-UUCUCCGAACGUGUCACGUTT-3'; antisense, 5'-ACGUGA-CACGUUCGAGAATT-3') were used as control. HT22 cells were pre-inoculated into 24-well plates. Subsequent transfection experiments were performed when the cells reached 50% confluence, and 2  $\mu$ L of siRNA and 1  $\mu$ L of Lipo3000 (ThermoFisher, USA) were added to 50  $\mu$ L of Opti-Mem medium (Gibco, USA) and incubated at 37 °C for 10 min, followed by the addition of 350  $\mu$ L of high-sugar DMEM medium to the mix and then added to the pre-laid cells. After transfection for 6 h, the medium was replaced with a complete medium, adding 2  $\mu$ M ZnCl<sub>2</sub> into ZnCl<sub>2</sub> group culture medium. After 42 h, the samples were collected for further analysis.

## 2.12. Quantification of malondialdehyde (MDA) and reduced glutathione (GSH) content

The cells were digested using trypsin; after washing with PBS twice, the cells were added to 300  $\mu$ L of PBS and subsequently crushed using an ultrasonic cell crusher at 300 W. This process was repeated four times, with a 30 s interval for each 5 s. Animal tissues were mixed with PBS at a ratio of 1 mL per 0.1 g and then ground using a tissue grinder. The tissues were then crushed four times with an ultrasonic cell crusher at 300 W, with a 30 s interval for each 5 s. Hippocampal tissue was processed in the same steps as above after grinding. Finally, the levels of MDA and reduced GSH in the serum, hippocampus and cells were measured according to the manufacturer's instructions for the MDA assay kit (Beyotime, China) and the reduced GSH assay kit (Nanjing Jiancheng Biotech, China), respectively.

## 2.13. Determination of intracellular Zn<sup>2+</sup> content

Cells were seeded onto polylysine-coated 12-well plates before transfection or stimulation with H<sub>2</sub>O<sub>2</sub>. After 48 h of transfection or 72 h of H<sub>2</sub>O<sub>2</sub> stimulation, the culture medium was removed, and the cells were washed with PBS. Subsequently, a 5  $\mu$ g/mL Zinpyr-1 solution (Santa Crus, USA) was added to the cells, which were incubated in a cell culture incubator for 30 min. Following incubation, the cells were detached and harvested using EDTA-free trypsin before centrifugation at 1000 rpm for 5 min. Next, 1 mL of PBS was added to resuspend the cells. The mixture was centrifuged at 1000 rpm for 5 min, and the process was repeated twice. The cells were resuspended by adding 500  $\mu$ L of PBS solution. Lastly, cell fluorescence intensity was measured using a flow cytometer at a wavelength of 488 nm.

### 2.14. Detection of $Zn^{2+}$ content in cell culture medium by inductively coupled plasma mass spectrometry (ICP-MS)

The cell culture medium was collected and centrifuged at 1000 rpm for 5 min, and 250  $\mu$ L of the upper culture medium was obtained for detection. Standard solutions were prepared at concentrations of 1, 2, 5, and 10 ppb. The cell culture supernatant was diluted 50-fold with the working solution. ICP-MS was used to measure the  $Zn^{2+}$  content in the cell culture medium.

### 2.15. Statistical analysis

Statistical analysis was conducted using SPSS 21.0 software (IBM, USA). The T-test was used to compare the two groups of data, while a one-way analysis of variance (ANOVA) was used to compare the three groups of data against each other. Statistical significance was set at  $p < 0.05$ . The results were presented as the mean  $\pm$  standard deviation (SD).

## 3. Results

### 3.1. MIA injection induced TMJ-OA

Macroscopic observation of the TMJ joints revealed defects on the articular surface of condyle and articular cartilage in all MIA

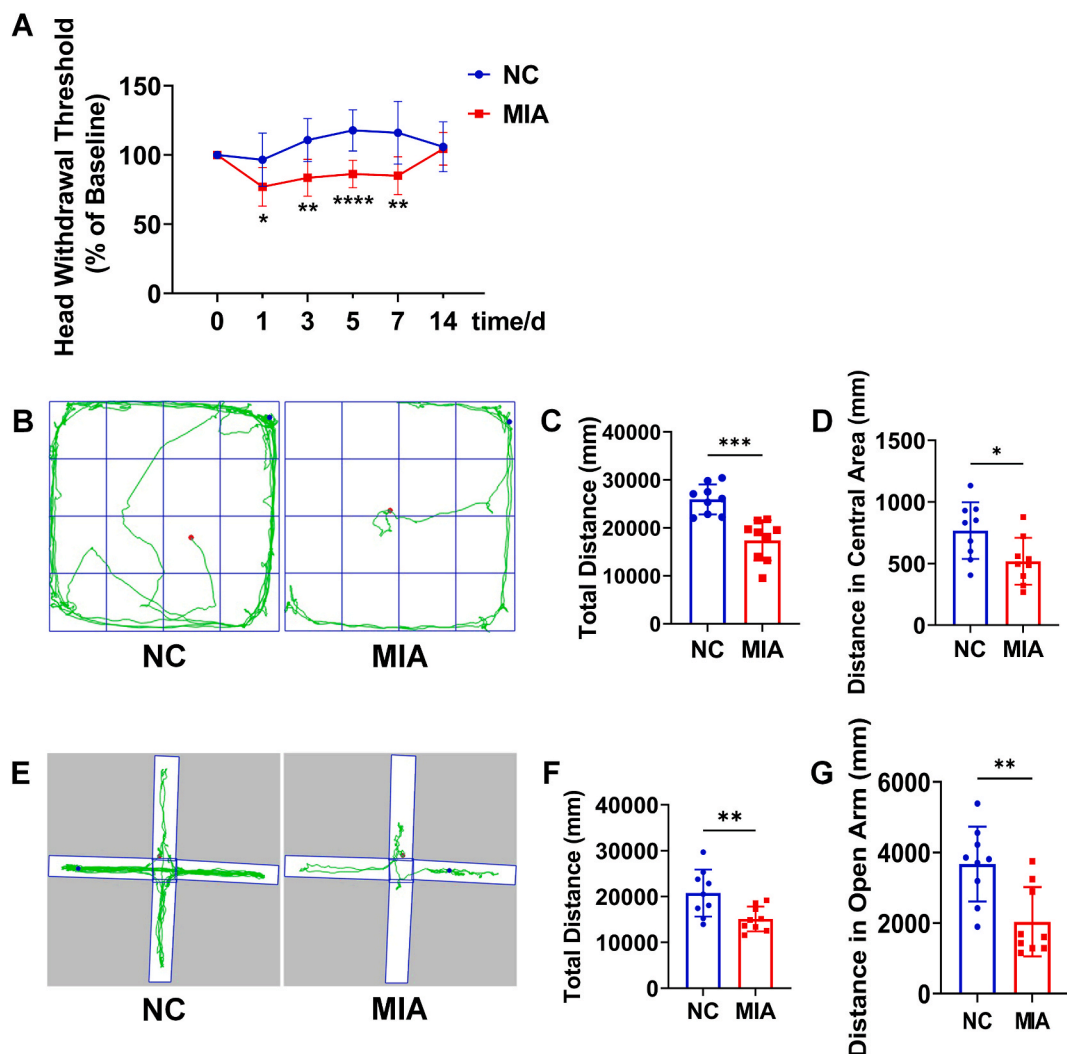


**Fig. 2.** TMJ-OA induced pain and anxiety-like behavior in rats.

(A) HWT (% of BL) of rats in NC group and MIA group from day 0 to day 14. (B) Rat movement trajectory in the OFT. (C) The total distance covered by rats in the OFT. (D) Distance covered by rats in the center area. (E) Rat motion trajectory in the EPM. (F) Total distance covered by rats in the EPM. (G) Distance covered by rats in the open arm. All data were mean  $\pm$  SD,  $n = 9$ , \* $p < 0.05$ , \*\* $p < 0.01$ , \*\*\* $p < 0.001$  vs. NC.

groups. In contrast, the NC group exhibited relatively smooth surface with cartilage integrity and no notable defects (Fig. 1D). HE staining of the sagittal sections of the rat TMJ condyles indicated that the condylar cartilages of healthy rats in the NC group manifested a consistent alignment of multilayer chondrocytes, comprising four unique layers: fibrous, proliferative, hypertrophic, and calcified cartilage layers. Six weeks after MIA injection, distinct lesions were evident in the condylar cartilage of rats in the MIA group, namely, a partial defect on the condylar cartilage surface, reduced and irregular chondrocyte arrangement, cartilage fibrosis, thinning or disappearance of the hypertrophic layer, disordered cell layers, and severe discontinuity (Fig. 1E). Safranin O-fast green staining revealed that the condylar cartilage proteoglycans of rats in the MIA group were significantly less than those in the NC group (Fig. 1F). The qRT-PCR results showed that Col2a1, Aggrecan mRNA expression in condylar cartilage of the MIA group was lower than that of the NC group (Fig. 1G and I), and MMP13 mRNA expression was elevated (Fig. 1H). Although not statistically significant ( $p=0.0764$ ), the relative expression of ADAMTS5 mRNA increased (Fig. 1J). Immunofluorescence of condylar cartilage showed decreased expression of Collagen II protein and increased expression of MMP13 protein in the MIA group compared to the NC group (Fig. 1K).

### 3.2. TMJ-OA induced pain and anxiety-like behavior in rats

HWT levels in rats were recorded using the Electric VonFrey to reflect mechanical sensitivity in the TMJ region. HWT did not differ at BL between the NC and MIA groups. In the first 7 days after MIA injection, the HWT of rats in the MIA group was lower than that of the NC group. HWT of rats in MIA group returned to BL level on day 14 (Fig. 2A).

We observed whether the rats showed behavioral changes in OFT and EPM at 2w, 4w, and 6w after injection of MIA. By the second week, there was no discernible difference in the performance of rats in the OFT and EPM tests (SFig. 1A–F). And by the fourth week, rats in the MIA group exhibited a reduction in movement distance only in the central area of the OFT, and no other differences were observed in the behavioral manifestations of either the OFT or EPM tests (SFig. 1G–L). While at 6w significant differences in movement trajectories were observed between rats in the NC and MIA groups during the OFT. The total travel distance of the MIA group was shorter than that of the NC group. Similarly, rats in the MIA group traveled shorter distances in the central area (Fig. 2B–D). Significant differences in the movement trajectories of the rats between the NC and MIA groups were also observed during the EPM. Throughout the observation period, the total distance traveled by the MIA group significantly decreased. Additionally, the MIA group

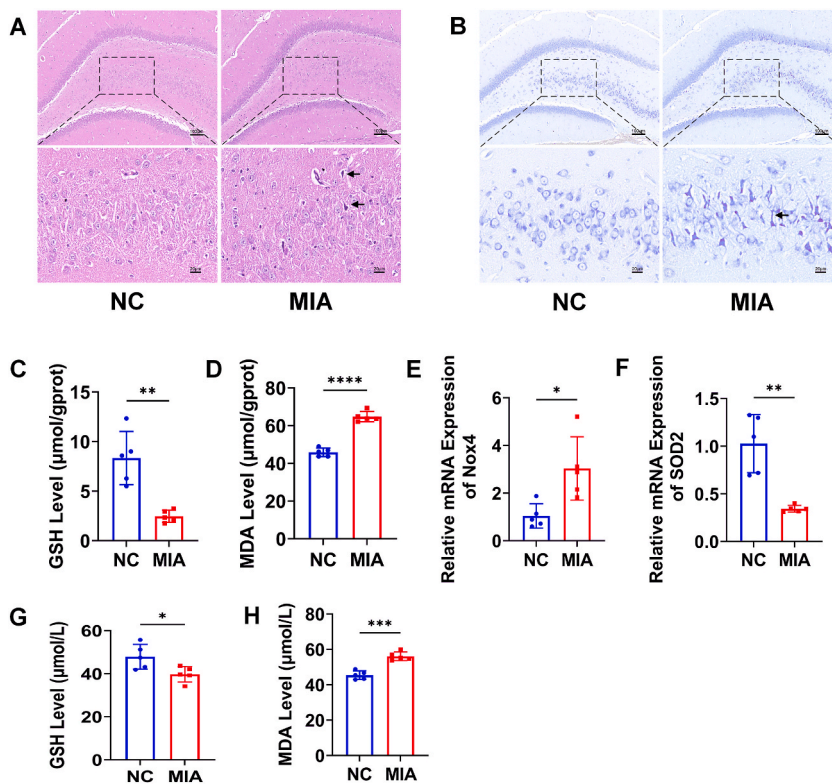


**Fig. 3.** TMJ-OA caused hippocampal neuron injury and oxidative stress in rats.

(A) HE staining of the hippocampus; injection of MIA leads to nuclear pyknosis of neurons, indicated by arrows. (B) Nissl staining of the hippocampus; injection of MIA leads to unclear structure, decreased number of neuronal bodies, and irregular-shaped neurons, indicated by arrows. (C and D) Content of reduced GSH and MDA in hippocampus tissue. (E and F) Relative mRNA expression of Nox4 and SOD2 in hippocampus tissue. (G and H) Contents of reduced GSH and MDA in rat serum. All data were mean  $\pm$  SD,  $n = 5$ , \* $p < 0.05$ , \*\* $p < 0.01$ , \*\*\* $p < 0.001$ , \*\*\*\* $p < 0.0001$  vs. NC.

demonstrated significantly shorter distance traveled in the open arms than those of their matched NC group (Fig. 2E–G). Thereby it could be concluded that the experimentally established TMJ-OA model rats exhibited changes in anxiety-like behavior.

### 3.3. TMJ-OA caused hippocampal neuron injury and oxidative stress in rats

HE staining showed that the number of hippocampal neurons was larger and more neatly arranged in the NC group with normal hippocampal structure and even staining. The number of hippocampal neurons was reduced, nuclear pyknosis was evident, and the intercellular spaces were enlarged in the MIA group (Fig. 3A). Nissl staining showed clear and abundant Nissl bodies with deep color in

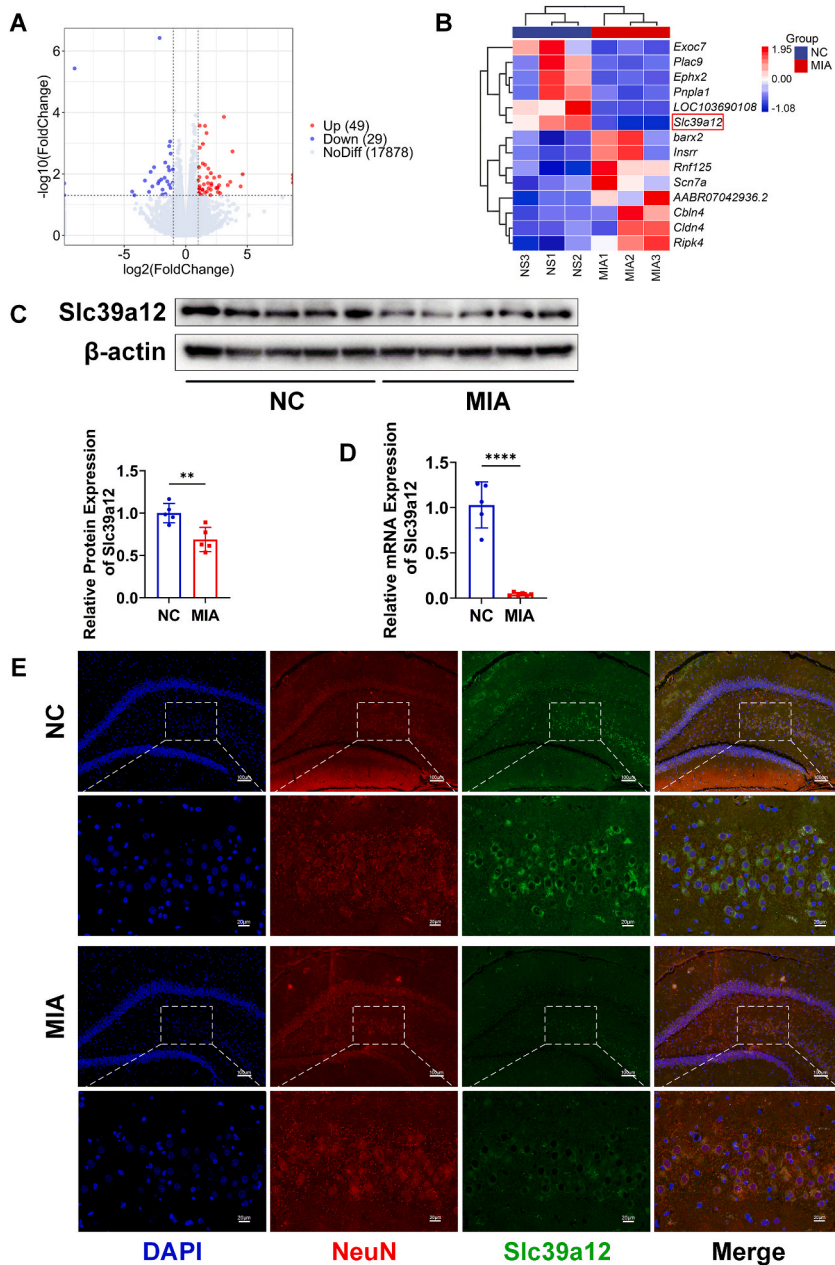


**Fig. 4.** TMJ-OA reduced Slc39a12 expression in hippocampal neurons. (A) Volcano plot of two groups (NC and MIA) of DEGs. The left blue dot signifies mRNA that expression significantly decreased in the MIA group, while the right red dot signifies mRNA that expression significantly increased in the MIA group. (B) Top 14 DEGs with Basemean >50,  $|\log_2\text{-FoldChange}| > 2$ , significant  $p$ -value <0.05. (C and D) Relative protein and mRNA expression of Slc39a12 in hippocampal tissue. (E) Immunofluorescence staining of NeuN (red) and Slc39a12 (green) in hippocampal tissue. All data were mean  $\pm$  SD,  $n = 5$ , \*\* $p < 0.01$ , \*\*\*\* $p < 0.0001$  vs. NC. (For interpretation of the references to color in this figure legend, the reader is referred to the Web version of this article.)

the NC group, while unclear structure, irregularly-shaped neuronal cell bodies and reduced number of Nissl bodies were detected in the MIA group. (Fig. 3B). Compared to the NC group, the reduced GSH content of the hippocampus and serum was significantly reduced (Fig. 3C and G) and MDA content was markedly increased (Fig. 3D and H) in the MIA group. The mRNA expression of NADPH oxidase (Nox) 4 increased in the hippocampus tissue of the MIA group (Fig. 3E), whereas the mRNA expression of superoxide dismutase (SOD) 2 was reduced (Fig. 3F). These results suggested increased oxidative stress in hippocampus of rats in the MIA group.

### 3.4. TMJ-OA reduced *Slc39a12* expression in hippocampal neurons

Compared to the NC group, 49 genes were upregulated and 29 genes downregulated in the MIA group (Fig. 4A). Further screening of the above differentially expressed genes (DEGs) under the conditions of  $\text{baseMean} > 50$ ,  $|\log_2\text{FoldChange}| > 2$  and a significant  $p$ -value  $< 0.05$  resulted in the discovery of 14 DEGs (Fig. 4B). We screened 14 genes and verified 13 of them by expanding the sample

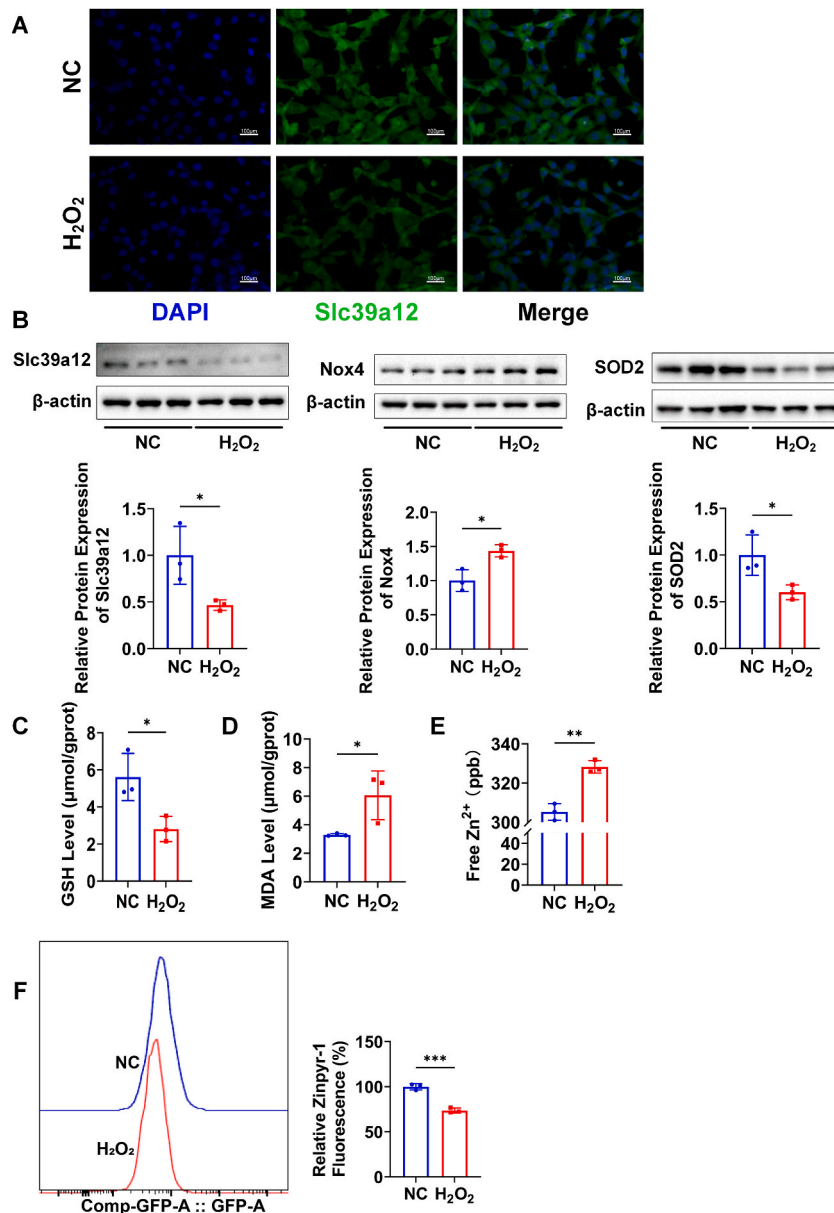


**Fig. 5.** *Slc39a12* expression was downregulated and oxidative stress was upregulated in HT22 cells exposed to H<sub>2</sub>O<sub>2</sub>. (A) Relative protein expression of *Slc39a12* in HT22. (B) Relative protein expression of *Slc39a12*, Nox4, and SOD2 in HT22. (C and D) Content of reduced GSH and MDA in TH22. (E) Zn<sup>2+</sup> content in HT22 cells' culture medium. (F) Flow cytometric analysis of HT22 cells stained with Zinpyr-1. All data were mean  $\pm$  SD,  $n = 3$ , \* $p < 0.05$ , \*\* $p < 0.01$ , \*\*\* $p < 0.001$  vs. NC.

size, except for the AABR07042936.2 gene, which is not expressed in humans. The mRNA expression levels of Ripk4, Insrr, Cbln4 and LOC103690108 genes were increased in the hippocampus of the MIA group (SFig. 2A–D), while the mRNA expression of Exoc7, Ephx2 and Slc39a12 genes were decreased (SFig. 2E and F, Fig. 4D). The changes of Ripk4, Insrr, Cbln4, Ephx2 and Slc39a12 expression were consistent with the results of RNA-seq. Based on a literature review demonstrating the role of Slc39a12 in neuronal development and oxidative stress, Slc39a12 was selected as the study target. Western blott showed that Slc39a12 protein expression in hippocampus of the MIA group were reduced compared to those in the NC group (Fig. 4C). The immunofluorescence results not only confirmed the decreased expression of Slc39a12 in hippocampus of rats in the MIA group but demonstrated that Slc39a12 was colocalized with the neuronal marker NeuN, indicating its neuronal expression (Fig. 4E).

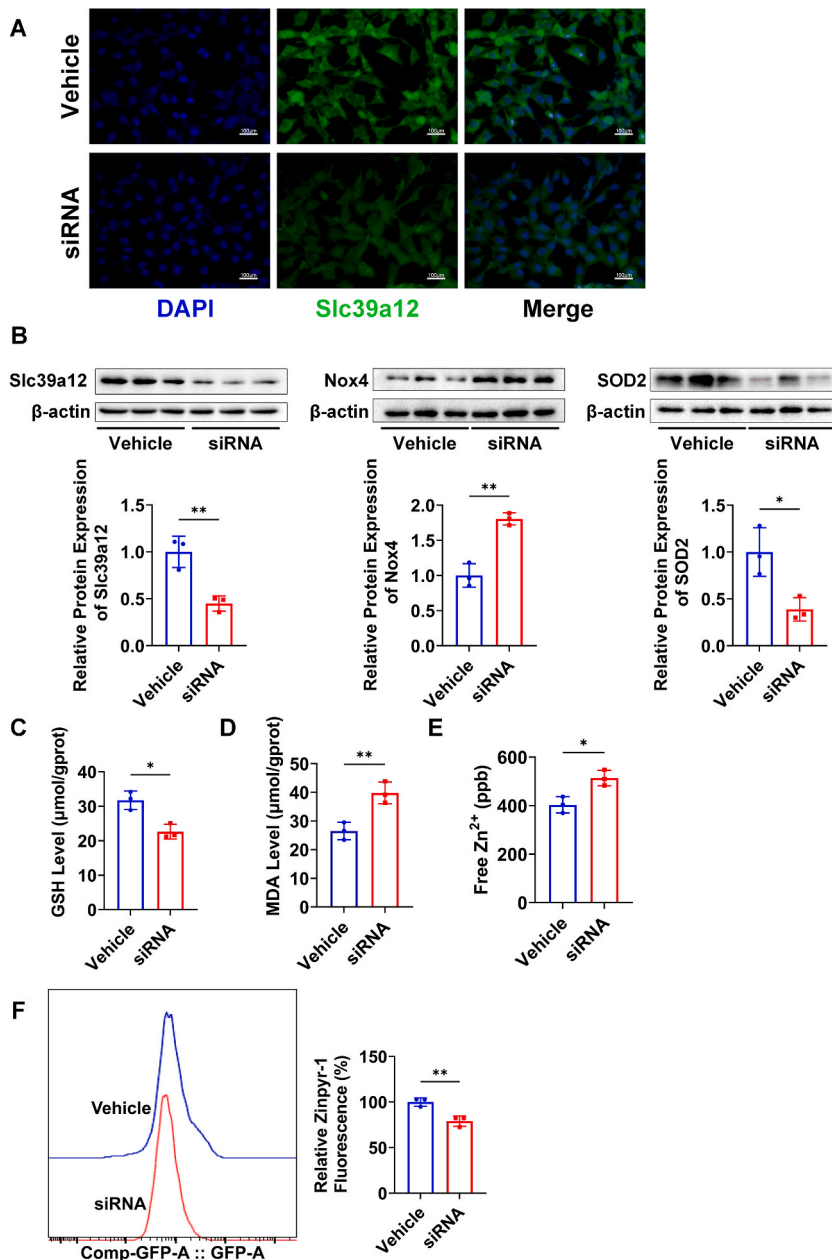


**Fig. 6.** Slc39a12 knockdown increased oxidative stress in HT22 cells.

(A) Relative protein expression of Slc39a12 in HT22 cells. (B) Relative protein expression of Slc39a12, Nox4, and SOD2 in HT22. (C and D) Content of reduced GSH and MDA in HT22 cells. (E) Zn<sup>2+</sup> content in HT22 cells' culture medium. (F) Flow cytometric analysis of HT22 cells stained with Zinpyr-1. All data were mean ± SD, n = 3, \*p < 0.05, \*\*p < 0.01, vs. Vehicle.

### 3.5. Slc39a12 expression was downregulated and oxidative stress was upregulated in HT22 cells exposed to H<sub>2</sub>O<sub>2</sub>

The expression of Slc39a12 decreased in HT22 cells after exposure to H<sub>2</sub>O<sub>2</sub> for 72 h (Fig. 5A and B). Concomitantly, Nox4 expression in HT22 cells increased, whereas superoxide dismutase 2 (SOD2) expression decreased after exposure to H<sub>2</sub>O<sub>2</sub> (Fig. 5B). Additionally, the reduced GSH content of HT22 cells decreased, whereas the MDA content increased after exposure to H<sub>2</sub>O<sub>2</sub> (Fig. 5C and D). Slc39a12, a member of the zinc transporter family, facilitates extracellular Zn<sup>2+</sup> transport into cells. After exposure to H<sub>2</sub>O<sub>2</sub> for 72 h, the concentration of Zn<sup>2+</sup> in the culture medium of HT22 cells increased (Fig. 5E). Simultaneously, the fluorescence intensity produced by the combination of Zinpyr-1 and Zn<sup>2+</sup> in HT22 cells decreased, pointing to a reduction in intracellular Zn<sup>2+</sup> concentration (Fig. 5F).

### 3.6. Slc39a12 knockdown increased oxidative stress in HT22 cells

In order to knock down the expression of Slc39a12, siRNA and control (Vehicle) were transfected into HT22 cells in this study. A significant reduction in Slc39a12 protein expression in HT22 cells was detected 48 h after siRNA transfection (Fig. 6A and B). Moreover, the concentration of Zn<sup>2+</sup> in the culture medium of HT22 cells increased following siRNA transfection (Fig. 6E). The fluorescence intensity produced by the intracellular Zinpyr-1/Zn<sup>2+</sup> complex decreased simultaneously, implying a reduction in intracellular Zn<sup>2+</sup> concentration (Fig. 6F). In HT22 cells, siRNA transfection resulted in decreased SOD2 expression and increased Nox4 expression (Fig. 6B). Slc39a12 knockdown led to a decline in reduced GSH content and an increase in MDA content in HT22 cells

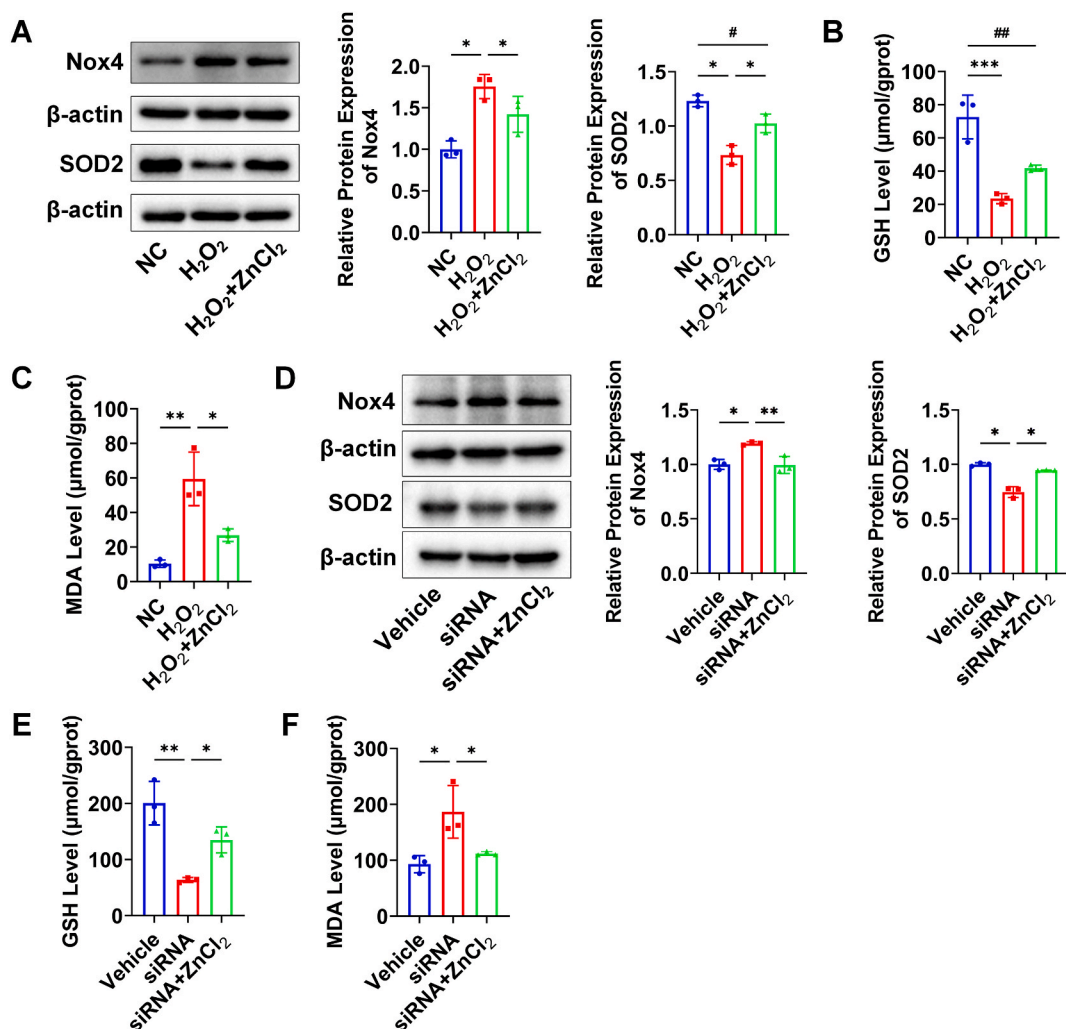


**Fig. 7.** ZnCl<sub>2</sub> treatment alleviated oxidative stress caused by Slc39a12 deficiency in HT22 cells.

(A) Relative protein expression of Nox4, and SOD2 in HT22 cells. (B and C) Content of reduced GSH and MDA in HT22 cells. (D) Relative protein expression of Nox4, and SOD2 in HT22 cells. (E and F) Content of reduced GSH and MDA in HT22 cells. All data were mean ± SD, n = 3, \*p < 0.05, \*\*p < 0.01 vs. H<sub>2</sub>O<sub>2</sub> or siRNA; #p < 0.05, ##p < 0.01 vs. NC.

(Fig. 6C and D). These findings indicate that reduced Slc39a12 expression may increase oxidative stress levels.

### 3.7. ZnCl<sub>2</sub> treatment alleviated oxidative stress caused by Slc39a12 deficiency in HT22 cells

The Western Blot results showed that treatment of HT22 cells with ZnCl<sub>2</sub> alleviated up-regulation of Nox4 induced by H<sub>2</sub>O<sub>2</sub> and restored expression of SOD2 (Fig. 7A). Measurements of cellular reduced GSH levels showed that ZnCl<sub>2</sub> treatment had a tendency to restore reduced GSH levels, although not statistically different from cells treated with H<sub>2</sub>O<sub>2</sub> alone (Fig. 7B). In addition, ZnCl<sub>2</sub> was able to suppress MDA levels in the H<sub>2</sub>O<sub>2</sub> environment (Fig. 7C). The addition of ZnCl<sub>2</sub> after knockdown of Slc39a12 showed that ZnCl<sub>2</sub> decreased the protein expression of Nox4, increased the protein expression of SOD2 (Fig. 7D), restored the level of reduced GSH, and down-regulated the level of MDA compared with the knockdown group (Fig. 7E and F).

## 4. Discussion

A strong correlation between TMJ injury and mood disorders has been demonstrated in previous studies, yet the underlying mechanism remains unrevealed. In this study, we established a TMJ-OA model by injecting MIA into the TMJ of rats. The rats thereafter showed decreased HWT and apparent TMJ-OA pain. Decreased synthesis and increased degradation of the condylar cartilage matrix were detected in rats six weeks after injection. Anxiety-like behavior and increased oxidative stress levels in the serum and hippocampus were observed in rats, which might be related to the reduced Slc39a12 expression.

The gross images of TMJ obtained in this study clearly showed articular cartilage defects. Notably, the TMJ histopathological findings revealed a discontinuous condylar cartilage layer of rats in the MIA group six weeks after MIA injection, with thinner even disappearing hypertrophic layer sometimes. Aggrecan and Collagen II are major proteins in cartilage matrix. The gene Col2a1 encodes Collagen II, while MMP13 and ADAMTS5 are matrix protein hydrolases involved in the degradation of components of the extracellular matrix. The results of O-fast green staining, qRT-PCR and immunofluorescence indicated local condylar cartilage thickness and cartilage matrix proteoglycan levels were significantly reduced. These findings conform to those of the previous research, indicating that the MIA injection into TMJ could effectively induce lesions similar to the clinical and experimental observations [19–22].

Classic behavioral tests, such as OFT and EPM, detect animal emotions through the conflict between their desire to explore and the fear of opening up to an unfamiliar environment and high degree [23]. When animals experience anxiety-like emotions, their desire for exploration decreases, leading to changes of behaviors in the OFT and EPM. Animals with anxiety induced by either chronic unpredictable mild stress (CUMS) or chronic restraint stress model usually display reduced movement and time spent in the central area in OFT, and exhibit decreased total movement and distance in the open arm in the EPM as well [24,25]. The TMJ-OA model established in the present study by injecting MIA into the TMJ of rats showed reduced total and central area moving distances in OFT and decreased total and open arm moving distances in EPM. These changes induced anxiety-like behavior, which aligned with the findings of previous study. Injecting complete Freund's adjuvant (CFA) into the TMJ of rats to simulate TMD pain resulted in decreased exploratory behavior, as indicated by fewer open arm entries and less time spent in the open wall during EPM experiments, less time spent in the bright area during light-dark box tests, and smaller shuttle number [26]. These findings suggest that CFA injection induces anxiety-like behavior in rats. Some researchers evaluated the emotions in OFT and EPM experiments via creating a TMJ-OA rat model through unilateral anterior crossbite (UAC). Two weeks after UAC, the total traveling distance in the central area significantly decreased in OFT. Both the time spent in the open arm of EPM and the number of entries into the arm decreased, suggesting that the TMJ-OA rat model via UAC also exhibited decreased exploratory behavior with anxiety-like tendencies [27]. Consistent with the findings in rodent models, patients with TMD tend to be more anxious and/or depressed than asymptomatic controls [28].

The correlation between TMD and altered levels of systemic oxidative stress in the clinical setting has been gradually confirmed by several studies of different populations diagnosed with TMD, which indicate increased 8-hydroxydeoxyguanosine and MDA, and decreased total anti-oxidant status in patients [29,30]. Reduced GSH is a major nonenzymatic antioxidant that scavenges free radicals, GSH level determines the antioxidant capacity of body, while the levels of MDA indirectly reflect the severity of the free radical attacks. The similar upregulation of MDA and down-regulation of GSH in rat serum was detected in our MIA intra-articular injection rat model, accompanied by articular cartilage defects anxiety often features a decrease in the organism's antioxidant capacity [31]. A clinical study found that serum levels of oxidative stress were higher in patients afflicted with multiple sclerosis, and the hospital anxiety and depression scale confirmed that anxiety scores were higher in the affected population. Subsequently, antioxidant N-acetylcysteine reduced the anxiety scores of the patients. It was also shown in animal research that the intraperitoneal administration of Edaravone, a free radical scavenger, ameliorated the anxiety-like behavior of mice after the use of a chronic social defeat stress approach [32–34].

The hippocampus is composed of large densely-arranged pyramidal neurons, which is crucial for memory and emotional information processing. Pathological results showed that the hippocampal neurons in the MIA group were damaged, nuclear pyknosis occurred, and Nissl bodies were reduced compared with the NC group in our study. Similarly, in a previous study, neuronal pyknosis and decreased Nissl bodies were observed in hippocampus of the anxious and depressed mice subjected to CUMS [35]. Nox4 is a member of NADPH oxidase family, widely expressed in all brain regions, functioning as a major source of endogenous ROS production [36]. As one of the major antioxidant enzymes that scavenge ROS, SOD2 plays an important role in protecting cells from oxygen-free radical poisoning [37]. Compared with the NC group, the reduced GSH content in hippocampus of the MIA group decreased, the MDA content increased, Nox4 expression increased, and SOD2 expression decreased, suggesting that TMJ-OA may induce increased oxidative stress levels. The hippocampus is particularly sensitive to oxidative stress and easily damaged, bringing forth anxiety. Traumatic brain injury causes anxiety-like behavior in rats presumably because of increased Nox4 expression in cortical tissue. Antioxidant Vorinostat effectively alleviates anxiety-like behavior of rats, accompanied by reduced level of Nox4 expression in the

cortical tissue [38]. Moreover, SOD2 expression can be reduced in hippocampus of CUMS model rats. Kaempferol exerts an anti-anxiety effect by upregulating SOD2 expression in hippocampal tissue [39]. Therefore, a high oxidative stress level of serum and subsequent injury of hippocampus may be the most probable reason for anxiety-like behaviors in our TMD rat model.

In the present study, TMJ-OA is a causative factor for increased oxidative stress and neuronal damage in hippocampus, resulting in anxiety-like behaviors of rats. To explore its specific molecular mechanisms, RNA-Seq was performed to investigate related genes. Members of the solute carrier 39 gene family encoding zinc transport proteins contribute to critical mechanisms, by which zinc homeostasis can be maintained across a wide range of species. Their main function is to promote the uptake of the extracellular environment and transport  $Zn^{2+}$  into cells [40]. A previous study showed that oxidative stress reduced the expression of zinc transporters in hepatocytes. After 72 h of hydrogen peroxide treatment for murine hepatocytes, the results demonstrated that hydrogen peroxide treatment altered the abundance of ZIPs protein, which might explain the reason for ethanol-induced hepatic zinc deficiency [41]. The zinc transporter ZIP12, which is encoded by the gene *Slc39a12*, is highly expressed in the vertebrate central nervous system [42]. *Slc39a12* mutations and deficiency may be linked to various genetic disorders, such as schizophrenia [43], autism [44], and Alzheimer's disease [45]. Strong et al. found that mitochondrial dysfunction was more severe in *Slc39a12* KO N2a cells than that in the control group, and ROS level was markedly up-regulated. Simultaneously, the neurite outgrowth of the induced nerves into differentiated cells was blocked. Overexpression of SOD2 or use of the antioxidant  $\alpha$ -tocopherol, MitoQ, and MitoTEMPO could effectively ameliorate the neurite shortening caused by *Slc39a12* knockdown [45].

Given the increased oxidative stress levels observed in the hippocampal tissue of rats in the MIA group in our experiments,  $H_2O_2$  was used to stimulate mouse hippocampal neuronal cells HT22 in vitro. As expected, in accord with in vivo experiment, together with the increased cellular oxidative stress levels, the protein expression of *Slc39a12* decreased, accompanied with decreased zinc influx. To explain further, the present in vitro study explored the role of *Slc39a12* via constructing a siRNA to knock down the expression of *Slc39a12* in HT22 cells, the intracellular  $Zn^{2+}$  concentration and cellular aggravate oxidative status accompany by reduced *Slc39a12* expression levels. Consistent with the previous report on spermatogonia C18–4 cells, which indicated that ZIP12 protects spermatogonia from oxidative stress during spermatogenesis [46]. Therefore, our study demonstrates that the ZIP12 deficiency induced by oxidative stress in hippocampus can lead to a decrease in zinc-associated antioxidant activity, thereby aggravating injury in turn.

Whereafter, we supplemented the culture medium with  $ZnCl_2$ , which could reverse the damage of hydrogen peroxide treatment or *Slc39a12* knockdown to HT22 cells. Zinc is essential for normal brain function. Zinc deficiency during early brain development can result in malformations, whereas Zinc deficiency in later brain development can impair multiple functions [47]. Zinc-deficient rats might experience anxiety-like behavior. Meanwhile, Timm's staining in hippocampus also decreased, and the intracellular calcium signaling activity in hippocampal slices was more than that in the control group [48]. Other studies also produced similar results that a lower dose of Zinc combined with standard anxiolytic and antidepressant drugs showed potentiating effect on rats with anxiety, depression and psychosis [49,50]. It should be clarified that we are conscious of the limitation in our vitro study. Thus, additional studies in vivo, such as *Slc39a12* over-expression and knock-down in hippocampus, are required to understand the precise role of *Slc39a12* in the TMJ-OA rat model related anxiety.

In conclusion, this study demonstrates that MIA intra-articular injection induced cartilage damage, imbalance of cartilage anabolism and catabolism. TMJ-OA may cause pain and anxiety-like behavior in rats, accompanied by hippocampal neuron injury and oxidative stress in serum and hippocampus. It may be attributed to the loss of *Slc39a12* and a decrease in  $Zn^{2+}$  content in neurons, bringing about increased oxidative stress levels and the ultimate neuronal damage, which can be relieved by Zinc supplement.

## Ethics statement

All procedures followed the care standards for laboratory animals and had been approved by the Laboratory Animal Ethics Committee of Anhui Medical University (LLSC20221097).

## Consent for publication

All authors consented for publication.

## Funding

This work was supported by the Research Fund of Anhui Institute of Translational Medicine [2022zhyx-C85]; 2022 Disciplinary Construction Project in School of Dentistry, Anhui Medical University [2022xkfyts08]; and Postgraduate Innovation Research and Practice Program of Anhui Medical University [YJS20230054].

## CRediT authorship contribution statement

**Zhenguo Shen:** Writing – original draft, Methodology, Investigation, Formal analysis, Data curation. **Chenyu Fan:** Methodology, Investigation, Formal analysis, Data curation. **Chunmeng Ding:** Visualization, Validation. **Mengyue Xu:** Writing – original draft. **Xian Wu:** Writing – original draft, Methodology. **Yuanyin Wang:** Project administration, Funding acquisition. **Tian Xing:** Writing – review & editing, Funding acquisition, Conceptualization.

## Declaration of competing interest

The authors declare that they have no known competing financial interests or personal relationships that could have appeared to influence the work reported in this paper.

## Acknowledgements

We express our gratitude to Associate Professor Liang Jing of the School of Psychiatry and Psychology at Anhui Medical University for his assistance and guidance in the animal behavior experiments, Dr. Chao Li of the School of Pharmacy at Anhui Medical University for their assistance in the experimental design, and Professor Deyong Chu of the School of Basic Medicine at Anhui Medical University for sponsoring TH22 cells. Some of the content depicted in the graphic abstract is sourced from Servier Medical Art, which is provided by Servier and licensed under a Creative Commons Attribution 3.0 unported license.

## Appendix A. Supplementary data

Supplementary data to this article can be found online at <https://doi.org/10.1016/j.heliyon.2024.e26271>.

## References

- [1] L.F. Valesan, C.D. Da-Cas, J.C. Réus, A.C.S. Denardin, R.R. Garanhani, D. Bonotto, E. Januzzi, B.D.M. de Souza, Prevalence of temporomandibular joint disorders: a systematic review and meta-analysis, *Clin. Oral Invest.* 25 (2) (2021) 441–453, <https://doi.org/10.1007/s00784-020-03710-w>.
- [2] A.M. Velly, S.M. Elsaraj, J. Botros, F. Samim, Z. der Khatchadourian, M. Gornitsky, The contribution of pain and disability on the transition from acute to chronic pain-related TMD: a 3-month prospective cohort study, *Front Pain Res (Lausanne)* 3 (2022) 956117, <https://doi.org/10.3389/fpain.2022.956117>.
- [3] M. Maślak-Bereś, J.E. Loster, A. Wiczorek, B.W. Loster, Evaluation of the psychoemotional status of young adults with symptoms of temporomandibular disorders, *Brain Behav* 9 (11) (2019) e01443, <https://doi.org/10.1002/brb3.1443>.
- [4] B. Paniagua, L. Pascal, J. Prieto, J.B. Vimort, L. Gomes, M. Yatabe, A.C. Ruellas, F. Budin, S. Pieper, M. Styner, E. Benavides, L. Cevidades, Diagnostic Index: an open-source tool to classify TMJ OA condyles, *Proc. SPIE-Int. Soc. Opt. Eng.* 10137 (2017), <https://doi.org/10.1117/12.2254070>.
- [5] J. Li, K. Ma, D. Yi, C.D. Oh, D. Chen, Nociceptive behavioural assessments in mouse models of temporomandibular joint disorders, *Int. J. Oral Sci.* 12 (1) (2020) 26, <https://doi.org/10.1038/s41368-020-00095-0>.
- [6] C.K. Ward, R.G. Gill, R.S. Liddell, J.E. Davies, Umbilical cord stem cell lysate: a new biologic injectate for the putative treatment of acute temporomandibular joint inflammation, *J. Inflamm. Res.* 16 (2023) 4287–4300, <https://doi.org/10.2147/jir.S420741>.
- [7] G. Isola, L. Perillo, M. Migliorati, M. Matarese, D. Dalessandri, V. Grassia, A. Alibrandi, G. Matarese, The impact of temporomandibular joint arthritis on functional disability and global health in patients with juvenile idiopathic arthritis, *Eur. J. Orthod.* 41 (2) (2019) 117–124, <https://doi.org/10.1093/ejo/cjy034>.
- [8] N. Su, Y. Liu, X. Yang, J. Shen, H. Wang, Association of malocclusion, self-reported bruxism and chewing-side preference with oral health-related quality of life in patients with temporomandibular joint osteoarthritis, *Int. Dent. J.* 68 (2) (2018) 97–104, <https://doi.org/10.1111/idj.12344>.
- [9] R.J. Gatchel, J.P. Garofalo, E. Ellis, C. Holt, Major psychological disorders in acute and chronic TMD: an initial examination, *J. Am. Dent. Assoc.* 127 (9) (1996) 1365–1370, <https://doi.org/10.14219/jada.archive.1996.0450>, 1372, 1374.
- [10] Y.J. Liou, Y.M. Bai, S.J. Tsai, T.J. Chen, M.H. Chen, W.L. Lo, Bidirectional associations of temporomandibular joint disorders with major depressive and anxiety disorders, *J. Evid. Base Dent. Pract.* 23 (2) (2023) 101860, <https://doi.org/10.1016/j.jebdp.2023.101860>.
- [11] D. Manfredini, A. Bandettini di Poggio, E. Cantini, L. Dell'Osso, M. Bosco, Mood and anxiety psychopathology and temporomandibular disorder: a spectrum approach, *J. Oral Rehabil.* 31 (10) (2004) 933–940, <https://doi.org/10.1111/j.1365-2842.2004.01335.x>.
- [12] D. Wang, Y. Qi, Z. Wang, A. Guo, Y. Xu, Y. Zhang, Recent advances in animal models, diagnosis, and treatment of temporomandibular joint osteoarthritis, *Tissue Eng., Part B* 29 (1) (2023) 62–77, <https://doi.org/10.1089/ten.TEB.2022.0065>.
- [13] I. Takahashi, T. Matsuzaki, M. Hosoi, Long-term histopathological developments in knee-joint components in a rat model of osteoarthritis induced by monosodium iodoacetate, *J. Phys. Ther. Sci.* 29 (4) (2017) 590–597, <https://doi.org/10.1589/jpts.29.590>.
- [14] S.Y. Yun, Y. Kim, H. Kim, B.K. Lee, Effective technical protocol for producing a mono-iodoacetate-induced temporomandibular joint osteoarthritis in a rat model, *Tissue Eng. C Methods* 29 (9) (2023) 438–445, <https://doi.org/10.1089/ten.TEC.2023.0066>.
- [15] G. He, Y. Li, H. Deng, H. Zuo, Advances in the study of cholinergic circuits in the central nervous system, *Ann Clin Transl Neurol* 10 (12) (2023) 2179–2191, <https://doi.org/10.1002/acn3.51920>.
- [16] M. Du, C. Wu, R. Yu, Y. Cheng, Z. Tang, B. Wu, J. Fu, W. Tan, Q. Zhou, Z. Zhu, E. Balawi, X. Huang, J. Ma, Z.B. Liao, A novel circular RNA, circIgf2bp2, links neural plasticity and anxiety through targeting mitochondrial dysfunction and oxidative stress-induced synapse dysfunction after traumatic brain injury, *Mol. Psychiatr.* 27 (11) (2022) 4575–4589, <https://doi.org/10.1038/s41380-022-01711-7>.
- [17] L.W. Swanson, Brain maps 4.0-Structure of the rat brain: an open access atlas with global nervous system nomenclature ontology and flatmaps, *J. Comp. Neurol.* 526 (6) (2018) 935–943, <https://doi.org/10.1002/cne.24381>.
- [18] T. Xing, Y. Liu, H. Cheng, M. Bai, J. Chen, H. Ji, M. He, K. Chen, Ligature induced periodontitis in rats causes gut dysbiosis leading to hepatic injury through SCD1/AMPK signalling pathway, *Life Sci.* 288 (2022) 120162, <https://doi.org/10.1016/j.lfs.2021.120162>.
- [19] S. Cömert Kiliç, N. Kiliç, M.A. Sümbüllü, Temporomandibular joint osteoarthritis: cone beam computed tomography findings, clinical features, and correlations, *Int. J. Oral Maxillofac. Surg.* 44 (10) (2015) 1268–1274, <https://doi.org/10.1016/j.ijom.2015.06.023>.
- [20] L. Li, H. Shi, H. Xie, L. Wang, MRI assessment and histopathologic evaluation of subchondral bone remodeling in temporomandibular joint osteoarthritis: a retrospective study, *Oral Surg Oral Med Oral Pathol Oral Radiol* 126 (4) (2018) 355–362, <https://doi.org/10.1016/j.oooo.2018.05.047>.
- [21] M. Molinet, N. Alves, A. Vasconcelos, N.F. Deana, Comparative study of osteoarthritis induced by monoiodoacetate and papain in rabbit temporomandibular joints: macroscopic and microscopic analysis, *Folia Morphol (Warsz)* 79 (3) (2020) 516–527, <https://doi.org/10.5603/FM.a2019.0104>.
- [22] C.M. Tsai, J.W. Chai, F.Y. Wu, M.H. Chen, C.T. Kao, Differences between the temporal and mandibular components of the temporomandibular joint in topographic distribution of osseous degenerative features on cone-beam computerized tomography, *J. Dent. Sci.* 16 (3) (2021) 1010–1017, <https://doi.org/10.1016/j.jds.2020.12.010>.
- [23] M. Rosso, R. Wirz, A.V. Loretan, N.A. Sutter, C.T. Pereira da Cunha, I. Jaric, H. Würbel, B. Voelkl, Reliability of common mouse behavioural tests of anxiety: a systematic review and meta-analysis on the effects of anxiolytics, *Neurosci. Biobehav. Rev.* 143 (2022) 104928, <https://doi.org/10.1016/j.neubiorev.2022.104928>.
- [24] C. Wang, M.H. Zhu, N. Sun, W. Shen, N. Jiang, Q.S. Zhao, Y.X. Zhang, Y. Huang, W.X. Zhou, Isorhynchophylline ameliorates stress-induced emotional disorder and cognitive impairment with modulation of NMDA receptors, *Front. Neurosci.* 16 (2022) 1071068, <https://doi.org/10.3389/fnins.2022.1071068>.

- [25] Y.Y. Yin, Z.K. Lai, J.Z. Yan, Q.Q. Wei, B. Wang, L.M. Zhang, Y.F. Li, The interaction between social hierarchy and depression/anxiety: involvement of glutamatergic pyramidal neurons in the medial prefrontal cortex (mPFC), *Neurobiol Stress* 24 (2023) 100536, <https://doi.org/10.1016/j.yynstr.2023.100536>.
- [26] G.C. do Nascimento, C.R. Leite-Panissi, Time-dependent analysis of nociception and anxiety-like behavior in rats submitted to persistent inflammation of the temporomandibular joint, *Physiol. Behav.* 125 (2014) 1–7, <https://doi.org/10.1016/j.physbeh.2013.11.009>.
- [27] X. Liu, K.X. Zhou, N.N. Yin, C.K. Zhang, M.H. Shi, H.Y. Zhang, D.M. Wang, Z.J. Xu, J.D. Zhang, J.L. Li, M.Q. Wang, Malocclusion generates anxiety-like behavior through a putative lateral habenula-mesencephalic trigeminal nucleus pathway, *Front. Mol. Neurosci.* 12 (2019) 174, <https://doi.org/10.3389/fnmol.2019.00174>.
- [28] G.H. Gameiro, A. da Silva Andrade, D.F. Nouer, M.C. Ferraz de Arruda Veiga, How may stressful experiences contribute to the development of temporomandibular disorders? *Clin. Oral Invest.* 10 (4) (2006) 261–268, <https://doi.org/10.1007/s00784-006-0064-1>.
- [29] B. Ege, A.O. Kucuk, M. Kopal, I. Koyuncu, A. Gonel, Evaluation of serum prolidase activity and oxidative stress in patients with temporomandibular joint internal derangement, *Cranio* 39 (3) (2021) 238–248, <https://doi.org/10.1080/08869634.2019.1606987>.
- [30] D. Rodríguez de Sotillo, A.M. Velly, M. Hadley, J.R. Friction, Evidence of oxidative stress in temporomandibular disorders: a pilot study, *J. Oral Rehabil.* 38 (10) (2011) 722–728, <https://doi.org/10.1111/j.1365-2842.2011.02216.x>.
- [31] Q. Shen, W. Huang, Y. Qiu, S. Wang, B. Zhang, N. Sun, Q. Zhou, Bergapten exerts a chondroprotective effect in temporomandibular joint osteoarthritis by combining intestinal flora alteration and reactive oxygen species reduction, *Biomed. Pharmacother.* 167 (2023) 115525, <https://doi.org/10.1016/j.biopha.2023.115525>.
- [32] R. Dang, M. Wang, X. Li, H. Wang, L. Liu, Q. Wu, J. Zhao, P. Ji, L. Zhong, J. Licinio, P. Xie, Edaravone ameliorates depressive and anxiety-like behaviors via Sirt1/Nrf2/HO-1/Gpx4 pathway, *J. Neuroinflammation* 19 (1) (2022) 41, <https://doi.org/10.1186/s12974-022-02400-6>.
- [33] G. Khalatbari Mohseni, S.A. Hosseini, N. Majdinasab, B. Cheraghian, Effects of N-acetylcysteine on oxidative stress biomarkers, depression, and anxiety symptoms in patients with multiple sclerosis, *Neuropsychopharmacol Rep* 43 (3) (2023) 382–390, <https://doi.org/10.1002/npr2.12360>.
- [34] H. Wang, M. Jin, M. Xie, Y. Yang, F. Xue, W. Li, M. Zhang, Z. Li, X. Li, N. Jia, Y. Liu, X. Cui, G. Hu, L. Dong, G. Wang, Q. Yu, Protective role of antioxidant supplementation for depression and anxiety: a meta-analysis of randomized clinical trials, *J. Affect. Disord.* 323 (2023) 264–279, <https://doi.org/10.1016/j.jad.2022.11.072>.
- [35] R. Liu, H. Zhou, H. Qu, Y. Chen, Q. Bai, F. Guo, L. Wang, X. Jiang, H. Mao, Effects of aerobic exercise on depression-like behavior and TLR4/NLRP3 pathway in hippocampus CA1 region of CUMS-depressed mice, *J. Affect. Disord.* 341 (2023) 248–255, <https://doi.org/10.1016/j.jad.2023.08.078>.
- [36] D.W. Infanger, R.V. Sharma, R.L. Davison, NADPH oxidases of the brain: distribution, regulation, and function, *Antioxidants Redox Signal.* 8 (9–10) (2006) 1583–1596, <https://doi.org/10.1089/ars.2006.8.1583>.
- [37] W. Qiu, Q. Sun, N. Li, Z. Chen, H. Wu, Z. Chen, X. Guo, F. Fang, Superoxide dismutase 2 scavenges ROS to promote osteogenic differentiation of human periodontal ligament stem cells by regulating Smad3 in alveolar bone-defective rats, *J. Periodontol.* (2023), <https://doi.org/10.1002/jper.23-0469>.
- [38] Y. Lu, Y. Chen, S. Xu, L. Wei, Y. Zhang, W. Chen, M. Liu, C. Zhong, HDAC inhibitor attenuates rat traumatic brain injury induced neurological impairments, *Heliyon* 9 (8) (2023) e18485, <https://doi.org/10.1016/j.heliyon.2023.e18485>.
- [39] H.Y. Li, J. Wang, L.F. Liang, S.Y. Shen, W. Li, X.R. Chen, B. Li, Y.Q. Zhang, J. Yu, Sirtuin 3 plays a critical role in the antidepressant- and anxiolytic-like effects of kaempferol, *Antioxidants* 11 (10) (2022), <https://doi.org/10.3390/antiox11101886>.
- [40] C. Ye, G. Lian, T. Wang, A. Chen, W. Chen, J. Gong, L. Luo, H. Wang, L. Xie, The zinc transporter ZIP12 regulates monocrotaline-induced proliferation and migration of pulmonary arterial smooth muscle cells via the AKT/ERK signaling pathways, *BMC Pulm. Med.* 22 (1) (2022) 111, <https://doi.org/10.1186/s12890-022-01905-3>.
- [41] Q. Sun, Q. Li, W. Zhong, J. Zhang, X. Sun, X. Tan, X. Yin, X. Sun, X. Zhang, Z. Zhou, Dysregulation of hepatic zinc transporters in a mouse model of alcoholic liver disease, *Am. J. Physiol. Gastrointest. Liver Physiol.* 307 (3) (2014) G313–G322, <https://doi.org/10.1152/ajpgi.00081.2014>.
- [42] W. Chowanadisai, D.M. Graham, C.L. Keen, R.B. Rucker, M.A. Messerli, Neurulation and neurite extension require the zinc transporter ZIP12 (slc39a12), *Proc. Natl. Acad. Sci. U. S. A.* 110 (24) (2013) 9903–9908, <https://doi.org/10.1073/pnas.1222142110>.
- [43] E. Scarr, M. Udawela, M.A. Greenough, J. Neo, M. Suk Seo, T.T. Money, A. Upadhyay, A.I. Bush, I.P. Everall, E.A. Thomas, B. Dean, Increased cortical expression of the zinc transporter SLC39A12 suggests a breakdown in zinc cellular homeostasis as part of the pathophysiology of schizophrenia, *NPJ Schizophr* 2 (2016) 16002, <https://doi.org/10.1038/npschz.2016.2>.
- [44] N. Krumm, T.N. Turner, C. Baker, L. Vives, K. Mohajeri, K. Witherspoon, A. Raja, B.P. Coe, H.A. Stessman, Z.X. He, S.M. Leal, R. Bernier, E.E. Eichler, Excess of rare, inherited truncating mutations in autism, *Nat. Genet.* 47 (6) (2015) 582–588, <https://doi.org/10.1038/ng.3303>.
- [45] M.D. Strong, M.D. Hart, T.Z. Tang, B.A. Ojo, L. Wu, M.R. Nacke, W.T. Agidew, H.J. Hwang, P.R. Hoyt, A. Bettaieb, S.L. Clarke, B.J. Smith, B.J. Stoeker, E. A. Lucas, D. Lin, W. Chowanadisai, Role of zinc transporter ZIP12 in susceptibility-weighted brain magnetic resonance imaging (MRI) phenotypes and mitochondrial function, *Faseb. J.* 34 (9) (2020) 10702–10725, <https://doi.org/10.1096/fj.202000772R>.
- [46] X. Zhu, C. Yu, W. Wu, L. Shi, C. Jiang, L. Wang, Z. Ding, Y. Liu, Zinc transporter ZIP12 maintains zinc homeostasis and protects spermatogonia from oxidative stress during spermatogenesis, *Reprod. Biol. Endocrinol.* 20 (1) (2022) 17, <https://doi.org/10.1186/s12958-022-00893-7>.
- [47] R. Sun, J. Wang, J. Feng, B. Cao, Zinc in cognitive impairment and aging, *Biomolecules* 12 (7) (2022), <https://doi.org/10.3390/biom12071000>.
- [48] A. Takeda, H. Tamano, F. Kan, H. Itoh, N. Oku, Anxiety-like behavior of young rats after 2-week zinc deprivation, *Behav. Brain Res.* 177 (1) (2007) 1–6, <https://doi.org/10.1016/j.bbr.2006.11.023>.
- [49] M. Joshi, M. Akhtar, A.K. Najmi, A.H. Khuroo, D. Goswami, Effect of zinc in animal models of anxiety, depression and psychosis, *Hum. Exp. Toxicol.* 31 (12) (2012) 1237–1243, <https://doi.org/10.1177/0960327112444938>.
- [50] A.J. Russo, Decreased zinc and increased copper in individuals with anxiety, *Nutr. Metab. Insights* 4 (2011) 1–5, <https://doi.org/10.4137/nmi.S6349>.